

Sensitivity of optimization of mid-infrared InAs/InGaSb laser active regions to temperature and composition variations

Michael E. Flatté

Department of Physics and Astronomy and Optical Science and Technology Center, University of Iowa, Iowa City, Iowa 52242

C. H. Grein

Department of Physics, University of Illinois, Chicago, Illinois 60607

H. Ehrenreich

Department of Physics and Division of Engineering and Applied Sciences, Harvard University, Cambridge, Massachusetts 02138

(Received 23 June 1997; accepted for publication 24 January 1998)

We calculate the temperature dependence of the threshold current density J_{th} in optimized (minimal J_{th}) and unoptimized InAs/InGaSb superlattices. We find that the threshold current density of the unoptimized superlattice is well described by $J_{\text{th}} \propto e^{T/T_0}$, with $T_0 \sim 32$ K from 25 to 275 K. This is the first microscopic calculation for these superlattices which indicates that J_{th} is well described by an empirical exponential form. In contrast, the threshold current density of the optimized superlattice is not well parametrized by a characteristic temperature T_0 . This superlattice is only optimized between 250 and 350 K, due to the sharp structure of the intersubband absorption spectrum. We also consider the effect on J_{th} of uncertainties in layer thicknesses. © 1998 American Institute of Physics. [S0003-6951(98)01812-9]

In mid-infrared semiconductor lasers, which are currently of great commercial and military interest, nonradiative processes dominate near room temperature and may lead to a rapidly increasing threshold current density (J_{th}) with increasing temperature. Nonradiative (Auger) events involving the recombination of a pair and the temporary excitation of another hole appear to dominate in lasers based on the InAs/InGaSb material system.^{1,2} Initial predictions for optimized InAs/InGaSb superlattices of nonradiative recombination rates lower than rates in bulk semiconductors motivated further exploration of this material system for use as a laser active region.³ In this letter we compare the temperature dependence of J_{th} for an optimized superlattice (designed for minimal J_{th} at 300 K), and another, unoptimized superlattice. A primary conclusion of this letter is that from 25 to 375 K the figure of merit T_0 , obtained from the empirical parametrization⁴ $J_{\text{th}}(T) \propto e^{T/T_0}$, describes the unoptimized superlattice well ($T_0 = 32$ K below 275 K, and $T_0 = 65$ K above 300 K), but completely fails to describe the optimized superlattice. This is the first calculation to indicate that for most InAs/InGaSb superlattices (i.e., unoptimized ones) J_{th} grows exponentially with temperature.

The unusual dependence on temperature for the optimized superlattice can be traced to band structure features within the valence band which diminish the intersubband absorption at the lasing energy (E_L) and also the Auger recombination rate. As the temperature increases, E_L decreases and the intersubband absorption per electron-hole pair (which, at fixed energy, is mostly independent of temperature) can increase or decrease depending on the local features of the intersubband absorption. A system optimized at a particular temperature has minimal intersubband absorption at the lasing energy and a minimum Auger rate for a given carrier density. A complementary investigation compared su-

perlattices with different layer thicknesses but the same band gap (E_g) at the same temperature. Here E_L remains the same but features in the intersubband absorption differ among the superlattices. The Auger rates depend sensitively on details of the band structure, but are relatively insensitive to variations in the layer thicknesses which are small but experimentally realizable: ± 3.5 Å for the InGaSb layer and ± 0.25 Å for the InAs layer.

The calculations of the band structures, threshold carrier densities (n_{th}) and J_{th} are described in detail in Refs. 5 and 6. In contrast to Refs. 5 and 6 band-gap changes with temperature and the effect of intersubband absorption (which must be minimized to optimize the laser performance) are included. For simplicity, many-body effects such as self-energy and collision contributions have been neglected. Based on considerations discussed in Refs. 5 and 6 we estimate the error in J_{th} as a factor of 3.

Parameters for the bulk constituents of the superlattices at 0 K are tabulated in Ref. 5. With the exception of the E_g , parameters of the InGaSb alloy are linearly interpolated and temperature independent. The temperature dependence of the bulk E_g for InAs is taken from Ref. 7, and for $\text{In}_{0.25}\text{Ga}_{0.75}\text{Sb}$ from Ref. 8. These energy gaps change by 57 and 80 meV, respectively, from 80 to 300 K.

Band structures at three different temperatures are shown in Fig. 1 for 12.5 Å InAs/39 Å $\text{In}_{0.25}\text{Ga}_{0.75}\text{Sb}$, which is optimized at 300 K. The most important intersubband transitions occur at the zone boundary in the growth direction. We show, therefore, two cross sections of the Brillouin zone; in the first, the momentum in the growth direction (K_{\perp}) increases from the zone center to the zone boundary with zero in-plane momentum (K_{\parallel}); in the second, K_{\parallel} increases from 0 to 0.1 Å⁻¹, while K_{\perp} remains at the zone boundary. Holes involved in the intersubband absorption originate in the HH1

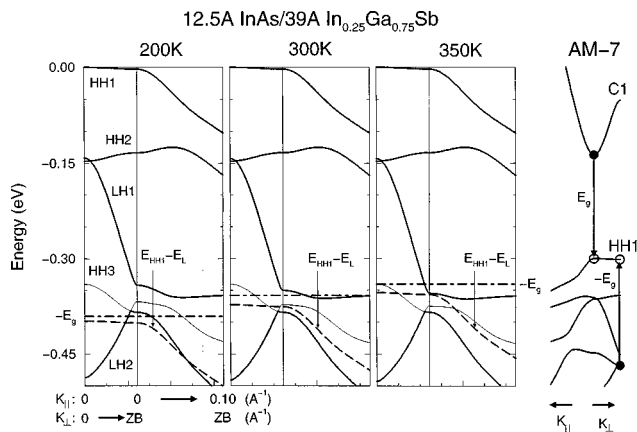


FIG. 1. Band structures for 12.5 Å InAs/39 Å In_{0.25}Ga_{0.75}Sb from 200 to 350 K. The dashed lines are the HH1 band rigidly shifted down by the lasing energy E_L , and are the important energies for intersubband absorption. The dot-dashed lines indicate the resonant energies for hole-hole Auger scattering at an energy gap E_g below the top of the valence band (taken to be the origin of the energy axis). The hole-hole Auger transition, AM-7, is shown schematically on the superlattice band structure on the far right.

subband. The energies E_L (corresponding to the lasing energy) below the HH1 subband are shown by the dashed lines. Intersubband absorption occurs at momenta where this dashed line crosses other bands. The temperature-dependence of the energy gap of the superlattice is comparable to that of the constituents, changing 60 meV from 100 to 300 K. The energy gap $E_g \sim E_L$ determines the resonant energy for Auger transitions within the valence subbands, and is indicated with a dot-dashed line on the band structures one energy gap below the top of the valence band.

If we neglect the HH3 subband (thin solid line), then in the temperature range 250–350 K the dashed line lies within a gap between the LH1 and LH2 subbands. As a result there is no Auger “resonance” and the intersubband absorption is minimal because of the lack of final states. At 300 K, as shown in Fig. 1, the LH1 and HH3 subbands are mostly inaccessible for Auger processes. Thus for this superlattice Auger processes which excite a hole (hole-hole Auger cf. Fig. 1) are weak and the dominant Auger processes at 300 K excite an electron (electron-electron Auger). In the unoptimized superlattice the LH1 and HH3 subbands are accessible for band-edge Auger processes. This in addition to the increased carrier density required to overcome intersubband absorption, leads to a larger hole-hole Auger rate than electron-electron Auger rate at 300 K.

Ignoring the HH3 subband is approximately correct, since the matrix elements between the HH1 and HH3 subbands are weak in the region of importance in the Brillouin zone. This picture is supported by Fig. 2, which shows the intersubband absorption spectrum, separated according to the final subband, for this superlattice at 300 K at the threshold carrier density. Since the valence band structure is not very sensitive to temperature (unlike E_g and E_L), we can visualize the effects of changing temperature on the intersubband absorption per electron-hole pair as primarily due to the changing E_L . The lasing energies at 200, 250, 300, and 350 K are indicated by arrows. Intersubband absorption at threshold (α_{int}) is only 30 cm⁻¹ at 300 K in this design, since E_L lies between two large features. At a temperature of 200 K, how-

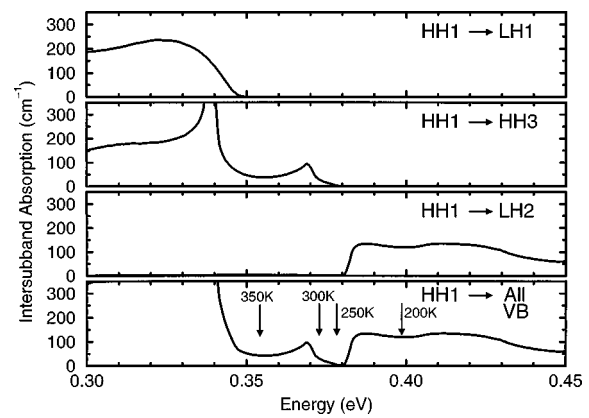


FIG. 2. Intersubband absorption as a function of photon energy for the 12.5 Å InAs/39 Å In_{0.25}Ga_{0.75}Sb superlattice at 300 K at the threshold carrier density. The top three plots show contributions from the three relevant final subbands, and the bottom plot is the total intersubband absorption. The arrows indicate the lasing wavelengths at 200–350 K.

ever, E_L lies within the higher-energy feature and α_{int} is 93 cm⁻¹. Since the intersubband absorption rises less quickly with density than the gain, by injecting more carriers it is usually possible to overwhelm the intersubband absorption. These additional carriers, however, increase the Auger recombination rate and lead to higher J_{th} .

α_{int} , n_{th} , and J_{th} for this optimized 12.5 Å InAs/39 Å In_{0.25}Ga_{0.75}Sb superlattice as a function of temperature are shown in Fig. 3. For comparison, the same three quantities for a 16.7 Å InAs/35 Å In_{0.25}Ga_{0.75}Sb superlattice are also shown. This latter superlattice was optimized based on 0 K band structure parameters,³ but is effectively unoptimized at 300 K. The differences between the two become quite noticeable above 200 K because the intersubband transition in the 16.7 Å InAs/35 Å In_{0.25}Ga_{0.75}Sb superlattice lies in the LH1 subband at these temperatures (cf. Fig. 1). At 300 K the optimized superlattice has a threshold current density a factor of 12 lower than the other superlattice.

Due to the anomalous behavior of the intersubband absorption of the optimized SL in the temperature range of 250–350 K, there is no reason to expect an empirical parametrization with a single T_0 to have any validity. In particular, for temperatures just below the optimized range, from 200 to 225 K, the T_0 exceeds 200 K, while above 300 K the T_0

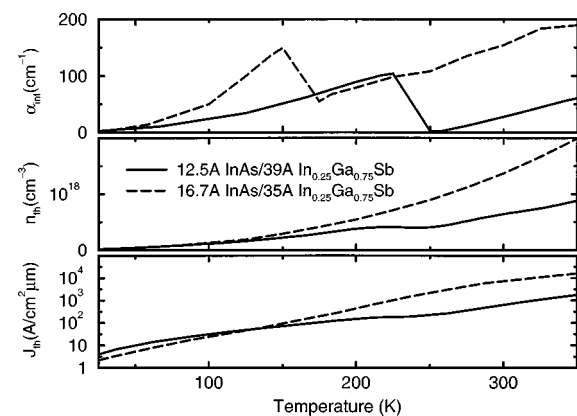


FIG. 3. Intersubband absorption at threshold (α_{int}), threshold carrier density (n_{th}), and threshold current density (J_{th}) as a function of temperature for two superlattices, one optimized from 250 to 350 K, and the other not.

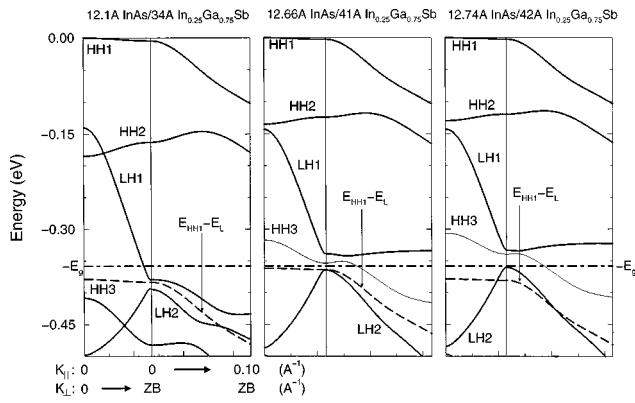


FIG. 4. Band structures for three superlattices with the same energy gap but different InGaSb layer thickness. Notations are as in Fig. 1.

value is 50 K. In contrast, a $T_0 = 32$ K for $T < 275$ K and $T_0 = 65$ K for $T > 300$ K describe the unoptimized superlattice well, due to the smoother character of the intersubband absorption at E_L .

It is interesting to note that the T_0 of the optimized SL above 300 K is lower than that of the unoptimized SL, even though the value of J_{th} is 12 times lower. This is due to the rapid rise in intersubband absorption in the optimized SL above 300 K. We note also that the relationship $J_{th} \propto T^{3/2}$ (Ref. 9) has been derived for a three-dimensional structure where intersubband absorption can be neglected and the radiative recombination rate dominates. This power law fits the unoptimized superlattice to 150 K, above which the large intersubband absorption makes J_{th} increase faster than $T^{3/2}$.

We have thus identified a key anomalous effect on the temperature dependence of J_{th} arising from nontrivial features within the band structure of the superlattice at the resonant energy. If the band structure at the resonant energy does not change much with temperature, then the T_0 parametrization may work. This is the case for bulk semiconductors and for InGaAsP 1.3 μm quantum well lasers.¹⁰ If we consider only the behavior of the Auger recombination rate with temperature for a fixed carrier density, then a related type of anomalous temperature dependence has been seen¹¹ in InAs and InAsSb/InAlAsSb multiple quantum wells, where there is a rough equality between E_g and the spin-orbit splitting Δ .¹² In the systems discussed in this letter, the anomalous changes in threshold carrier concentration due to the structure in the intersubband absorption have a more pronounced effect on the temperature dependence of J_{th} than the effects on the Auger rate for fixed carrier concentration.

As T varies the band structure features are roughly unchanged, but the relevant energies E_g and E_L change. We conclude by considering the complimentary case of changing the band structure features (by adjusting the layer thicknesses) and leaving E_g unchanged. Figure 4 shows the band structures of three superlattices at 300 K with the same band gap but different layer widths, indicating the important energies for intersubband absorption (dashed line) and the resonant energy for Auger recombination (dot-dashed line). The intersubband absorption should be smallest when the energies lie between LH1 and LH2. As shown in Fig. 5, n_{th} and J_{th} are smaller for InGaSb layer thicknesses less than 42 Å. When the layer thickness reaches 42 Å, the LH2 state is

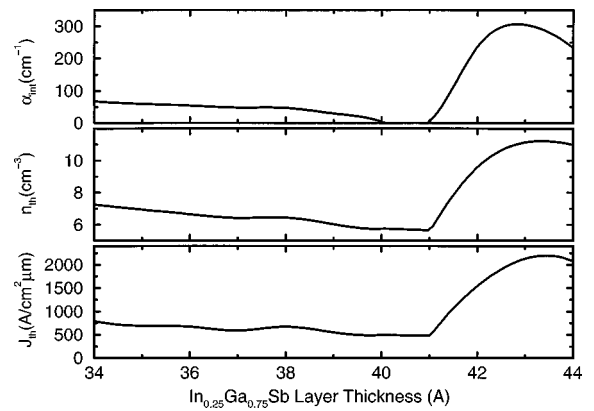


FIG. 5. Intersubband absorption at threshold, threshold carrier density, and threshold current density for a family of superlattices with the same energy gap but different InGaSb layer thicknesses.

resonant for intersubband processes from HH1, α_{int} jumps by 200 cm^{-1} , n_{th} doubles and J_{th} quadruples. The relative constancy of J_{th} from a InGaSb layer width of 34–41 Å suggests that within a superlattice this thickness must be controlled to within ± 3.5 Å. The band gap of the superlattice is much more sensitive to the InAs layer thickness, so J_{th} is roughly constant over a much shorter range of InAs layer thickness, from 12.1 to 12.66 Å. Therefore the InAs layer thickness must be controlled to within ± 0.25 Å, which is within the control of current molecular beam epitaxy technology.¹³

Note added in proof: During review we have become aware of related work by Bewley *et al.*¹⁴

The authors (H.E. and C.H.G.) would like to acknowledge support from DARPA under ONR Contract No. N00014-96-1-0887.

- ¹S. W. McCahon, S. A. Anson, D.-J. Jang, M. E. Flatté, T. F. Boggess, D. H. Chow, T. C. Hasenberg, and C. H. Grein, *Appl. Phys. Lett.* **68**, 2135 (1996).
- ²S. A. Anson, J. T. Olesberg, T. F. Boggess, T. C. Hasenberg, M. E. Flatté, and C. H. Grein (unpublished).
- ³C. H. Grein, P. M. Young, and H. Ehrenreich, *J. Appl. Phys.* **76**, 1940 (1994).
- ⁴G. P. Agrawal and N. K. Dutta, *Long Wavelength Semiconductor Lasers* (Van Nostrand, Reinhold, New York, 1986).
- ⁵M. E. Flatté, C. H. Grein, H. Ehrenreich, R. H. Miles, and H. Cruz, *J. Appl. Phys.* **78**, 4552 (1995).
- ⁶C. H. Grein, P. M. Young, M. E. Flatté, and H. Ehrenreich, *J. Appl. Phys.* **78**, 7143 (1995).
- ⁷H. H. Wieder and A. R. Clawson, *Thin Solid Films* **15**, 217 (1973).
- ⁸A. P. Roth, W. J. Keeler, and E. Fortin, *Can. J. Phys.* **58**, 560 (1980).
- ⁹For example, P. T. Landsberg, *Recombination in Semiconductors* (Cambridge University, New York, 1991), Eq. (4.5.22).
- ¹⁰D. A. Ackerman, P. A. Morton, G. E. Shtengel, M. S. Hybertsen, R. F. Kazarinov, T. Tanbun-Ek, and R. A. Logan, *Appl. Phys. Lett.* **66**, 2613 (1995).
- ¹¹J. R. Lindle, J. R. Meyer, C. A. Hoffman, F. J. Bartoli, G. W. Turner, and H. K. Choi, *Appl. Phys. Lett.* **67**, 3153 (1995).
- ¹²First predicted for GaSb by A. Haug, *J. Phys. C* **20**, 1293 (1987).
- ¹³Such a statement is only meaningful when the layer thicknesses are interpreted as average thicknesses of layers with atomically abrupt interfaces.
- ¹⁴W. W. Bewley *et al.* (unpublished).